ELSEVIER

Materials Science and Engineering B58 (1999) 130–133

MATERIALS SCIENCE & ENGINEERING B

DLTS analysis of nickel–hydrogen complex defects in silicon

M. Shiraishi [a,c,*], J.-U. Sachse [a], H. Lemke [b], J. Weber [a]

[a] *Max-Planck-Institut für Festkörperforschung, Heisenbergstrasse 1, D-70569 Stuttgart, Germany*
[b] *TU Berlin, Institut für Werkstoffe der Elektronik, Jebensstrasse 1, D-10623 Berlin, Germany*
[c] *Sony Corporation Research Center, 174 Fujitsuka-cho, Hodogaya-ku, Yokohama 240, Japan*

Abstract

The results of a deep level transient spectroscopy (DLTS) study of nickel–hydrogen complexes in n- and p-type silicon are presented. Hydrogen is incorporated by wet-chemical etching. After etching, eleven electrically active Ni–H related levels are observed. Heat treatment enables us to investigate the thermal stability of Ni–H complexes. Possible structures of the Ni–H defects are proposed. © 1999 Elsevier Science S.A. All rights reserved.

Keywords: Hydrogen; Silicon; Transition metal; DLTS

1. Introduction

Hydrogen is known to form complexes with transition metals in Si (e.g. Au [1], Pd [2] and Pt [3]), which either introduce new levels in the band gap or passivate the deep levels of transition metals. In this study, we focus on isolated nickel and nickel–hydrogen complex defects in n- and p-type silicon. Although Ni is detrimental to device performance due to the fast diffusion and precipitate formation, there is little agreement in the literature concerning the nature of this impurity [4–6]. Evidence for several hydrogen induced electrically active Ni complexes in silicon is presented, their thermal stability is studied and possible structures of these complexes are discussed.

2. Experimental procedure

We used phosphorus- or boron-doped float zone or Czochralski (Cz) silicon. Doping of nickel is performed during the crystal growth in concentrations of about 10^{12} cm^{-3} or by diffusion at temperatures between 950 and 1050°C in concentrations of about 10^{14} cm^{-3}. Two sets of n- and p-type samples were used with different shallow donor/acceptor concentrations (10^{14} cm^{-3} and 10^{16} cm^{-3}). Samples could be cleaved from the Si rod which was doped during the float zone crystal growth. The cleaved samples allowed us to avoid the introduction of hydrogen in the samples. In our experiments hydrogen is introduced into the samples by wet chemical etching in a 1:2:1 mixture of HF, HNO_3 and CH_3COOH before evaporation of the Schottky contacts. The material for the Schottky contact is Au for n-type and Al for p-type.

The experimental setup in this study is a computerized lock-in DLTS system. The shallow dopant concentration profiles are determined by the capacitance-voltage (CV) method at 1 MHz. DLTS concentration profiling was used to determine the distribution of the deep levels. The profiles are calculated taking into account the nonuniform shallow dopant profiles due to hydrogen passivation of dopants.

3. Results

In Fig. 1 typical DLTS spectra of cleaved samples are shown: spectrum (a) is from an n-type sample and only the two levels of the substitutional Ni acceptor $Ni^{-/0}$ and double acceptor $Ni^{--/-}$ are observed; spectrum (b) is from a p-type sample, the single DLTS peak corresponds to the substitutional Ni donor $Ni^{0/+}$. The position of the Ni DLTS peaks coincides with the levels reported in the literature [4–6]. In Table 1 a summary of level positions and cross sections for all substitutional Ni levels is given. Spectrum (a) in Fig. 2 of an

* Corresponding author.

0921-5107/99/$ - see front matter © 1999 Elsevier Science S.A. All rights reserved.
PII: S0921-5107(98)00280-3

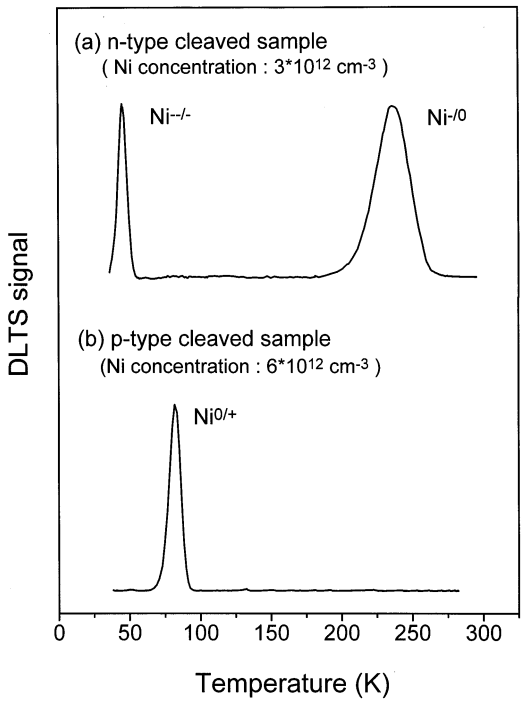

Fig. 1. DLTS spectra of cleaved samples; (a) cleaved sample of Ni-doped n-type Si; (b) cleaved sample of Ni-doped p-type Si.

n-type Si sample which was diffused with Ni is measured directly after wet-chemical etching. During the etching hydrogen is introduced and five new hydrogen related levels can be observed. We label the levels according to the peak temperatures [E(95), E(105), E(145), E(185), and E(270)] at an emission rate of 42 s^{-1}. Level position and electrical properties of the different DLTS peaks are summarized in Table 1. The level labeled A in [6] seems to be our level E(95). After annealing at 470 K for 1 h (Fig. 2(b)), the intensity of all the new hydrogen related peaks weakened. A heat treatment at 570 K for 2 h leads to an increase of $Ni^{-/0}$ and $Ni^{--/-}$ signals compared to those in the freshly etched sample. The decrease of the hydrogen related levels and the increase of the substitutional Ni levels with annealing suggests that all new hydrogen related levels belong to Ni–H complexes. A new DLTS peak (E(155)) appears after annealing at 470 K and another one (E(175)) at even higher annealing temperatures of 570 K (see Fig. 2(c)). The assignment of E(155) and E(175) to other Ni–H complexes is very speculative. Contamination of the samples by other impurities is a possibility which has to be studied in more detail in future. Our measurements indicate that Ni–H complexes in n-type Si are dissociated around 570 K and reactivation of the isolated Ni occurs.

In Fig. 3, typical DLTS spectra of a Ni-diffused p-type Si sample are shown. Wet chemical etching generates six new hydrogen related levels (Fig. 3(a)). Spectrum (b) is from the sample which was annealed at 500 K for 1 h. Almost all hydrogen-related peaks vanish and only one new level, H(140), appears. We annealed samples up to 600 K but H(140) still remains and no reactivation of the isolated Ni donor happens. It is therefore difficult to associate the new hydrogen related levels with Ni–H complexes from these measurements. Detailed measurements on differently prepared samples are underway to determine the Ni incorporation in the H complexes. From a comparison with the results on the n-type samples and the weakly Ni doped float zone samples we tentatively associate the six new levels to Ni–H complexes. Similar to n-type samples, we find that level H(140) is not Ni–H related. There is no reactivation of the substitutional Ni up to 600 K. This result could indicate a high stability of the

Table 1
The activation energy E_a, the capture cross section calculated by the extraporation of the Arrhenius plot σ_{ext}, the capture cross section by the variation of the filling pulse length σ_{fil}, the activation energy of the capture cross section E_b, the enthalpy H_a and the entropy factor X_s of Ni related levels

Level	E_a(eV)	σ_{ext}(cm^2)	σ_{fil}(cm^2)	E_b(eV)	H_a (eV)	X_s
$Ni^{--/-}$	$E_c-0.08$	4.2×10^{-14}	5.8×10^{-19} (45 K)	0.05	0.03	0.2
$Ni^{-/0}$	$E_c-0.39$	2.2×10^{-16}	4.4×10^{-17} (237 K)	0.08	0.31	0.1
$Ni^{0/+}$	$E_v+0.15$	4.3×10^{-15}	2.2×10^{-15}	0	0.15	2.2
H(50)	$E_v+0.08$	1.6×10^{-15}	1.1×10^{-15}	0	0.08	1.5
H(105)	$E_v+0.20$	2.6×10^{-15}	1.7×10^{-15}	0	0.20	1.5
H(160)	$E_v+0.32$	9.6×10^{-15}	9.9×10^{-17}	0	0.32	97
H(190)	$E_v+0.37$	6.5×10^{-15}	2.3×10^{-16}	0	0.37	28
H(235)	$E_v+0.47$	5.5×10^{-15}	3.7×10^{-16}	0	0.47	15
H(275)	$E_v+0.56$	5.3×10^{-15}	2.2×10^{-16}	0	0.56	24
E(95)	$E_c-0.15$	2.8×10^{-16}	4.8×10^{-18} (95 K)	0.02	0.13	5.1
E(110)	$E_c-0.16$	1.8×10^{-16}	1.4×10^{-17}	0	0.16	13
E(145)	$E_c-0.25$	6.6×10^{-16}	1.2×10^{-18}	0	0.25	550
E(185)	$E_c-0.35$	2.8×10^{-15}	1.8×10^{-18}	0	0.35	1600
E(270)	$E_c-0.52$	1.9×10^{-15}	7×10^{-16}	0	0.52	2.7

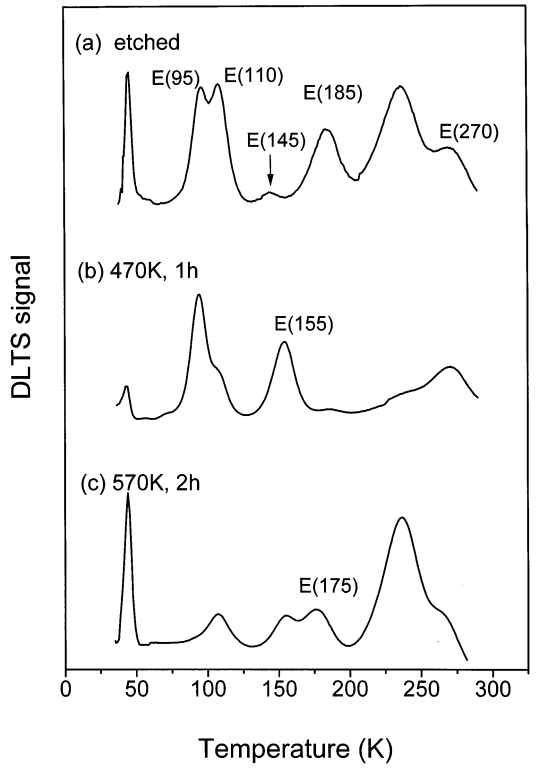

Fig. 2. DLTS spectra of Ni-diffused n-type Si: (a) after etching; (b) after annealing at 470 K for 1 h; (c) after annealing at 570 K for 3 h. The emission rate is $v_e = 42\ s^{-1}$, $V_r = -2$ V, $V_p = 0$ V. The DLTS signal scale of (a) is a half of that of (c), and so the intensities of isolated Ni levels in (c) are about twice as large as those of (a).

Ni–H complexes in p-type Si or more probable the complexing of substitutional Ni with other impurities.

In the determination of the capture cross sections, we use two different methods, the extrapolation of the Arrhenius plot to $T \rightarrow \infty$ and the variation of filling pulse length (T fixed). Furthermore, we investigated the activation energies of the capture cross sections, E_b. In n-type material, for example, the relationship between the emission coefficient and the capture cross section can be written as follows [7].

$$e_n = \sigma_n v_{th} N_c \exp\left(-\frac{\Delta G_n}{kT}\right), \quad (1)$$

where ΔG_n is the Gibbs free energy to excite an electron from a trap center to the conduction band and is described as $\Delta G_n = \Delta H_n - T\Delta S_n$ (ΔH_n enthalpy, ΔS_n entropy and T temperature). Eq. (1) can be rewritten as

$$e_n = \sigma_n X_s v_{th} N_c \exp\left(-\frac{\Delta H_n}{kT}\right), \quad (2)$$

where $X_s = \exp(\Delta S_n/k)$ is an entropy factor. If the capture cross section shows no temperature dependence, the difference of the capture cross sections determined by the two methods originates from the entropy factor. Our results for the capture cross section are shown in Table 1. For some levels σ is temperature dependent and E_b is not equal to zero.

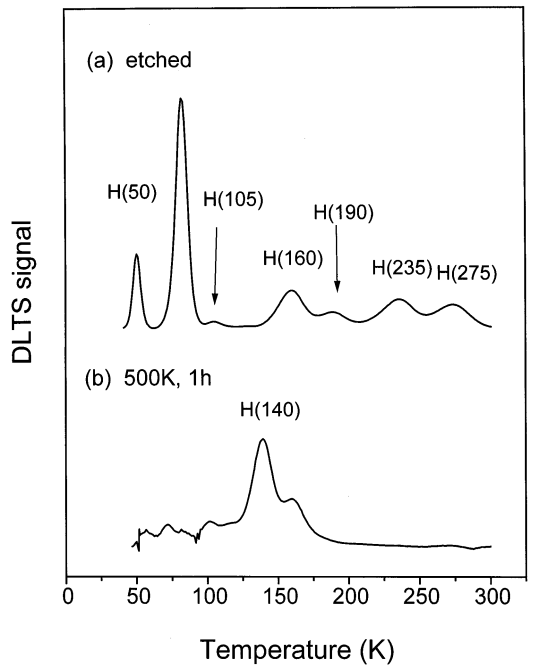

Fig. 3. DLTS spectra of Ni-doped p-type Si: (a) after etching; (b) after annealing at 500 K for 1 h.

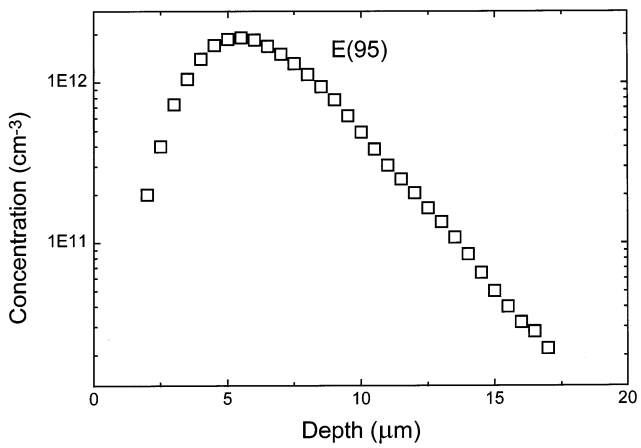

Fig. 4. A typical depth profile of the Ni–H related center E(95).

The properties of H(50) and H(105) are similar to those of Fe–B pairs and substitutional Cu, respectively. The activation energy of H(50) is however clearly smaller than that of Fe–B pair (0.10 eV [8]) and the activation energy of H(105) is also smaller than that of

Table 2
Penetration length L and possible structures of Ni–H complexes

Level	L (μm)	L_1/Li	I	Possible structure
E(95)	1.8 ± 0.05	2.1 ± 0.2	2	Ni–H_2
E(270)	3.7 ± 0.2	1	1	Ni–H
H(190)	1.0 ± 0.1	3.7 ± 0.7	3–4	Ni–$H_{3,4}$
H(235)	1.7 ± 0.1	2.2 ± 0.3	2	Ni–H_2
H(275)	1.4 ± 0.4	2.6 ± 0.4	2–3	Ni–$H_{2,3}$

substitutional Cu (0.23 eV [9]). Moreover the capture cross section of Cu is more than 1×10^{-14} cm^2 [9]. Therefore, H(50) can not be identified with the Fe–B pair and H(105) is certainly not related to substitutional Cu.

The concentration profiles of mobile hydrogen and hydrogen related complexes can be described by the following diffusion equations [10],

$$\frac{\partial[\mathrm{H}]}{\partial t} = D\frac{\partial^2[\mathrm{H}]}{\partial x^2} + V\frac{\partial[\mathrm{H}]}{\partial x} - \frac{[\mathrm{H}]}{\tau}, \quad (3)$$

$$\frac{\partial[A_i]}{\partial t} = V\frac{\partial[A_i]}{\partial x} + 4\pi D(r_{i-1}[A_{i-1}] - r_i[A_i])[\mathrm{H}], \quad (4)$$

where [H] is the concentration of mobile hydrogen, $[A_i]$ is the concentration of complexes, i is the number of hydrogen atoms, r_i is the radius of hydrogen, V is the etching velocity, D and τ are the diffusion coefficient and lifetime of mobile hydrogen, respectively. In the limit of the simplification discussed in [10], these equations are easily solved as $[A_i] \propto \exp(-ix/L)$. Here L is the penetration length. This solution shows the characteristic depth of penetration length is inversely proportional to the number of hydrogen atoms in the complexes. By fitting this equation to the measured defect distribution, possible structures can be derived. In samples with larger shallow dopant concentration, the depletion region is too narrow to investigate the distribution of defects. Therefore, only samples with lower concentrations of Ni (10^{12} cm^{-3}) and shallow dopants in the order of 10^{14} cm^{-3} were measured. In these samples, however, some Ni–H levels, which were found in the higher Ni doped samples, were not detected. In Fig. 4, a typical depth profile of the Ni–H complex (E(95)) is shown. It can be seen that the distribution of the complex exponentially decreases. From the model presented above the possible number of hydrogen atoms in the complexes can be determined from the penetration length L. A summary of all levels detected in the samples with low Ni concentration and a possible assignment to different Ni–H complexes is given in Table 2.

4. Summary

In summary, 11 new nickel–hydrogen related levels can be detected in Ni doped silicon after wet-chemical etching. In n-type Si, Ni–H complexes dissociate above 500 K. From the depth distribution of complexes an estimate for the number of H atoms involved in the complexes is given.

Acknowledgements

We thank H.-J. Queisser, T. Yamada and S. Watanabe for their encouragement during the course of this work. The authors would like to acknowledge the technical assistance of W. Heinz and W. Krause and thank B. Hammer for the sample preparation.

References

[1] E.Ö. Sveinbjörnsson, O. Engström, Phys. Rev. B 52 (1995) 4884.
[2] J.-U. Sachse, J. Weber, H. Lemke, Mat. Sci. Forum 258 (1997) 307.
[3] J.-U. Sachse, E.Ö. Sveinbjörnsson, W. Jost, J. Weber, Phys. Rev. B 55 (1997) 16176.
[4] S.J. Pearton, A.J. Tavendale, J. Appl. Phys. 54 (1983) 1375.
[5] H. Lemke, Mater. Sci. Forum 196–201 (1995) 683.
[6] H. Kitagawa, H. Nakashima, Jpn. J. Appl. Phys. 28 (1989) 305.
[7] D.K. Schroder, Semiconductor Material and Device Characterization, Wiley, New York, 1990.
[8] H. Nakashima, T. Sadoh, Mat. Res. Soc. Proc. 262 (1992) 555.
[9] S.D. Brotherton, J.R. Ayres, A. Gill, J. Appl. Phys. 62 (1987) 1826.
[10] O.V. Feklisova, N.A. Yarykin, Semicond. Sci. Technol. 12 (1997) 742.